Glass Europe Vol. 1 (2023) 55-66
https://doi.org/10.52825/glass-europe.v1i.890

Submitted: 17 Oct. 2023 | Accepted: 23 Nov. 2023 | Published: 06 Dec. 2023

Assessment of the Thermal Shock Resistance of Neodymium Doped Alumino-Phosphate Laser Glasses

Crystal Guillet[1], Rafael J. Jiménez-Riobóo[2], and Francisco Muñoz[1,*]

[1] Institute of Ceramics and Glass (CSIC), Spain

[2] Institute of Materials Science of Madrid (CSIC), Spain

* Correspondence: fmunoz@icv.csic.es

Abstract. The resistance to thermal shock is one of the main properties to be considered in the design of glasses for their application as high power and high energy laser glasses. Neodymium doped phosphate glasses have inherent spectroscopic advantages for their use as laser hosts, however, their rather low mechanical performance can be a limiting factor for their use. It is very important to characterise the thermo-mechanical resistance of proprietary phosphate glass compositions as laser glasses, however, it is not common to find systematic studies on the influence of glass composition on the thermal shock resistance in phosphate glasses, which is defined as the mechanical resistance of the material to the stresses generated by thermal fluctuations. This includes considering the elastic properties of the medium, its thermal conductivity, the coefficient of thermal expansion and the fracture toughness. In the present work we have studied these properties in a series of alumino-phosphate glasses doped with Nd_2O_3 as a function of the alumina content. The above properties have been determined by Brillouin spectroscopy, dilatometry and thermal diffusivity, while the fracture toughness has been approached by means of a theoretical model that uses the calculation of the energy necessary to create a new surface while a pre-existing crack progresses. The results showed that the calculated fracture toughness agrees with the one of similar commercial laser glass compositions, and that the thermal shock resistance calculated in the metaphosphate glasses increases with the addition of Al_2O_3.

Keywords: Laser Glasses, Phosphate Glasses, Neodymium, Mechanical Properties

1. Introduction

Rare earth doped phosphate glasses, and particularly Nd^{3+} doped, are nowadays some of the preferred laser hosts for high power and repetition systems. Despite the very well-known lower chemical durability and mechanical resistance of the phosphate glasses against the silicate ones, phosphate compositions have mostly been employed in fusion energy experiments, notably in the National Ignition Facility of the USA. Meanwhile the spectroscopic properties of the rare earth ions in laser glasses must be first optimised for their proper functionality, it is the control of the glass resistance under service, in all its broad sense, that will ultimately determine its ability to work as a laser host, very especially in the case of high power and repetition modes.

While in operation, the optical pumping process is followed by thermal changes across the glass slabs that become a source of stresses. On the one hand, it may produce undesired variation in the refractive index that is necessary to minimise by selecting athermal compositions with a variation of n with temperature of about half the coefficient of thermal

expansion [1]. On the other hand, crack formation and growth during manipulation, as well as mechanical loading and stresses generated from thermal variation, must be under control for the adequate performance and duration of the host. Thus, the fracture toughness and the so-called thermal shock resistance are the most important parameters to consider.

Using the definition by Kingery [2], the thermal shock resistance of a glass can be defined as the resistance to fracture under the stresses that develop when the material is submitted to a rapid change in temperature. Under such conditions, an elastic body will fracture after the stress overpasses a certain level. Thus, the resistance to develop stress at the surfaces will be proportional to the material ability to conduct heat and inversely proportional to the elastic modulus and coefficient of thermal expansion. The expression or figure of merit used to quantify the shock resistance in glasses can be written as:

$$R_S = \lambda \cdot (1-\nu) \cdot K_{Ic} / (E \cdot CTE) \quad (1)$$

Where λ is the thermal conductivity, ν the coefficient of Poisson, K_{Ic} the fracture toughness, E the elastic modulus and CTE the coefficient of thermal expansion. High values of thermal conductivity as well as low values of elastic modulus and coefficient of expansion are ideal for a high resistance to thermal shock, which will directly effect on avoiding the initiation of fracture.

The determination of the fracture toughness in glasses requires by far the most complicated experimental means and sample preparation in order to get reliable results without interference of the measuring method on the real effects of crack propagation. The theory behind the various existing methods of measuring fracture toughness in glasses has been well described in recent reviews such as in [3]. Attempts to determine the toughness by indentation measurements, however, may be possible but usually fail to provide realistic values because deformation and nucleation of defects take place before real crack propagation or even suffer of sub-critical crack propagation due to environmental humidity influence. Rouxel has recently shown that it is possible a theoretical calculation of the fracture toughness (K_{Ic}) through the energy that is necessary to create a new surface along with the propagation of a pre-existing flaw within the material [4], whose equations will be shown below.

The thermal shock resistance in phosphate glasses has only been studied in the compositions that have application as laser hosts, and the first studies of this property in phosphate laser glasses were reported by Cerqua *et al.*, whereby the authors evaluated the resistance of the surface of ion-exchanged glasses to cracking when submitted to temperature differences [5]. Some similar methodology was later employed by Jiang *et al.* in Er^{3+} doped phosphate glasses [6], however, although reports on properties of laser glasses have regularly mentioned the determined thermal shock resistance [1], [7], [8], there has not yet been systematic studies on the reasons by which this property is influenced by composition or structure. In this work, we present a study on the thermal-mechanical resistance of a series of alumino-phosphate glasses, for which the alumina content is increased and the metaphosphate compositional line maintained at the expense of reducing the amount of glass modifier elements, Na, K and Ba. All glasses have been doped with 1 mol % Nd_2O_3. The required properties necessary to obtain the thermal shock resistance of the glasses have been determined by dilatometry, thermal diffusivity and Brillouin spectroscopy and the fracture toughness of the glasses estimated through the theoretical model developed by Rouxel [4].

2. Experimental

Phosphate glasses were formulated with compositions $(15.5-5x/8)Na_2O$-$(15.5-5x/8)K_2O$-$(19-3x/4)BaO$-xAl_2O_3-$(50+x)P_2O_5$ (x=0, 2, 4, 6, 8 mol %) and all were doped with 1 % Nd_2O_3. This formulation makes the glasses to keep a constant ratio between Na_2O and K_2O of 1, and a constant ratio between $(Na_2O+ K_2O)/BaO$ of 1.625. Batches for 75 g of glass were obtained by mixing reagent grade chemicals, $(NH_4)H_2PO_4$ (*ACROS Organics*, 99+%), Na_2CO_3 (*Alfa*

Aesar, 99.5% min.), K_2CO_3 (*Sigma Aldrich*, ≥99%), Al_2O_3 (*Alfa Aesar*, 99.9%), $BaCO_3$ (Alfa Aesar, 99-101%) and Nd_2O_3 (Alfa Aesar, 99.99%) in stoichiometric amounts. They were thoroughly homogenised and then slowly calcined in porcelain crucibles, from room temperature up to 360ºC, with a rate of 0.5 ºC.min^{-1}, then kept overnight at that temperature and finally heated up to temperatures between 850 and 1100ºC depending on the composition to be melted for 1 h. The melts were poured on brass plates and left cooling freely to room temperature. About 7 g of the as-melted glasses were submitted to dehydroxylation by a second melting under a N_2 flow in a graphite mould using the procedure established previously by the authors in [9], and also employed for the alumino-phosphate glass with 4 mol % Al_2O_3 studied in [10]. The re-melting was done at 850ºC for 9 h in samples from 0 to 6 % Al_2O_3 and for 12 h for 8 and 10 %. The final obtained glasses between 0 and 8 % Al_2O_3 were very homogenous, bubble free and with no striae, thus having quite with good optical quality. Because the dehydroxylation re-melting ends with a cooling step inside the furnace at a free pace, any composition with a high tendency to devitrify make result in spontaneous crystallization, what happened for the 10 % Al_2O_3 glass. The X-Ray Diffraction analysis of that sample presented crystallized $Al(PO_3)_3$, as a result of the high content of alumina that progressively approached the aluminium metaphosphate composition with the reduction of all other modifiers.

The chemical composition of the dehydrated glasses was then analysed by X-ray Fluorescence Spectroscopy in a *PANalytical MagicX 2400* spectrometer using the pearl method of 0.3 g of glass with 5.5 g of $Li_2B_4O_7$.

The absorption coefficient of OH ions (α_{OH}) in the glasses was calculated by performing Fourier-Transformed Infrared Spectroscopy (FTIR), from 450 and 5000 cm^{-1}, in a Perkin-Elmer Spectrum 100 spectrometer using plane-parallel, mirror-like polished glass samples about 2 mm thick. The α_{OH} was obtained from the transmission value at 3000 cm^{-1} with respect to the maximum sample transmission at 5000 cm^{-1} using the relation $\alpha_{OH} = -\log(T_{3000}/T_{5000})/t$, being t the sample thickness.

The density was determined by the Archimedes method using ethanol as immersion liquid at room temperature; then the molar volume was calculated from the ratio between the molar mass of the glass analysed composition and its density.

Glass transition temperature and coefficient of thermal expansion (CTE) were determined from the dilation curves in a *Netzsch Gerätebau* model 420 PC/1 dilatometer, with a heating rate of 5 K.min^{-1}, in air, and after equipment calibration with an Al_2O_3 standard.

Heat capacity curves were obtained from determination of complete heat capacity curves between 20 and 500ºC by DSC, in a Discovery calorimeter from TA Instruments, at a heating rate of 10ºC.min^{-1} and recording three experiments per sample.

Elastic properties, Young's modulus, coefficient of Poisson and the refractive index were determined by high Resolution Brillouin Spectroscopy (HRBS), using the plane-parallel, mirror-like polished glass samples, following the experimental setup described in reference [11]. In order to obtain statistically relevant data, five points in different places of each sample were taken. 90A and backscattering (180) geometries were simultaneously used to measure sound velocity (v) from the Brillouin frequency shift, f, and the acoustic wave vector of the scattering geometries:

$$v^{90A} = \frac{f^{90A}\lambda_0}{\sqrt{2}} \; ; \; v^{180} = \frac{f^{180}\,\lambda_0}{2n} \qquad (2)$$

where λ_0 is the laser wavelength. The refractive index (at the laser wavelength of 532 nm) was obtained using the equation:

$$n = \frac{f^{180}}{f^{90A}\sqrt{2}} \quad (3)$$

The elastic properties are derived from the two independent elastic constants, c_{11} and c_{44}, related via the mass density to the longitudinal (v_L) and transverse (v_T) sound propagation velocities, respectively:

$$c_{11,44} = \rho \cdot v_{L,T}^2 \quad (4)$$

Thus, the corresponding Young's modulus (E) and Poisson's coefficient (ν) can be calculated from c_{11} and c_{44} [12]:

$$E = \rho\, v_T^2 \frac{(3v_L^2 - 4v_T^2)}{(v_L^2 - v_T^2)} \; ; \; \nu = \frac{(v_L^2 - 2v_T^2)}{(2v_L^2 - 2v_T^2)} \quad (5)$$

Thermal diffusivity measurements were performed by the laser pulse method in a thermaflash 2200 instrument from *Holometrix Inc. Thematest Division*, Cambridge, MA. (USA) on plane-parallel square samples of ca. 6.7 mm side and covered with gold and graphite layers to improve signal detection. The bottom side of the sample is heated homogeneously with a laser pulse at 1060 nm and 15 J power, so that the absorbed heat by the surface can be transmitted throughout producing an increase of temperature at the upper side and determined with an InSb infrared radiation detector. The thermal diffusivity can thus be calculated from the transmission of heat in the sample using the ASTM E 1461-92 and ISO/DIS 18755 norms with an error below 5 % and up to 7 measurements of thermal diffusivity were taken for each sample. Thereafter, the thermal conductivity (λ) is calculated with the equation:

$$\lambda = \rho \times C_p \times \alpha \text{ (in } W.K^{-1}.m^{-1}) \quad (6)$$

where ρ, C_p and α, are the density, heat capacity and diffusivity, respectively.

3. Results and discussion

Table 1 gathers the results of the analysed compositions for the dehydrated glasses containing from 0 to 8 mol % Al_2O_3, as well as the nominal and experimental O/P ratios and the absorption coefficient of hydroxyl ions in the glasses from the FTIR measurements. The calculation of O/P ratio has been done considering all analysed oxides, including the small amount of SiO_2 found in most samples, as due to dissolution from the crucible material when melting. However, all glasses present oxides contents within ± 0.5 mol % with respect to nominal compositions and O/P ratio remains slightly above 3 and very close to the nominal one. The O/P ratio must not be exactly 3 because of the small addition of 1 mol % Nd_2O_3. The analysed glass samples were those employed for the properties measurements that will be shown below.

***Table 1**. Relative content of oxides in mol % from the analysis by XRF of dehydrated glass samples, nominal and experimental O/P ratios and OH coefficient of absorption at 3000 cm^{-1}. Error in the determination of every element is given as the average deviation from the results in all glasses.*

Glass code	Na_2O ± 0.2	K_2O ± 0.1	BaO ± 0.5	Al_2O_3 ± 0.04	Nd_2O_3 ± 0.1	SiO_2 ± 0.04	P_2O_5 ± 0.4	Nom. O/P	Exp. O/P	α_{OH} (cm^{-1})
0Al	14.5	16	18.1	0	0.9	0.72	49.9	3.03	3.028	0.65
2Al	13.7	14.4	17	1.74	1	0.68	51.5	3.029	3.03	0.67
4Al	12	13.4	15.8	4.26	0.8	0	53.7	3.028	3.025	1.18
6Al	11.3	11.8	13.7	5.61	0.9	1.48	55.3	3.027	3.036	0.99
8Al	9.1	10.8	12.2	8.01	0.8	2.34	56.7	3.026	3.057	1.02

The calculated coefficient of absorption (α_{OH}) remains very low, near 1 cm^{-1} in all cases, and always below 2, as usually required for the rare-earth doped glasses in order to minimise the non-radiative relaxation processes that would otherwise produce important quenching of the Nd^{3+} fluorescence. The content of water in the glasses can thus be considered within the 100 ppm limit, which additionally contributes to a very high optical homogeneity for spectroscopy purposes.

Table 2 gathers the main properties measured in the glasses, thermal and elastic properties as determined by dilatometry, density, Brillouin spectroscopy, heat capacity curves and thermal diffusivity, that will later be used to calculate the thermal shock resistance of the glasses.

***Table 2**. Thermal and elastic properties of dehydrated glasses: glass transition temperature (T_g), coefficient of thermal expansion (CTE), density (d), refractive index (n), elastic modulus (E), coefficient of Poisson (ν), heat capacity (C_p) and thermal diffusivity (α).*

Glass code	T_g (ºC)	$CTE_{30\text{-}300ºC}$ ($x10^6$ K^{-1})	E (GPa)	ν	n	D ($g.cm^{-3}$)	C_p ($J.g^{-1}.ºC^{-1}$) at 27ºC	α ($x10^7$ $m^2.s^{-1}$)
0Al	318	20.38	41.68 ± 00.46	0.290 ± 0.005	1.5053 ± 0.0058	2.8860 ± 0.0200	0.5308 ± 0.0543	2.36 ± 0.04
2Al	349	17.99	43.46 ± 0.66	0.280 ± 0.003	1.5077 ± 0.0074	2.8827 ± 0.0149	0.5487 ± 0.0627	2.52 ± 0.04
4Al	379	15.96	46.72 ± 0.22	0.272 ± 0.002	1.5064 ± 0.0019	2.8503 ± 0.0027	0.5857 ± 0.0899	2.72 ± 0.03
6Al	413	14.68	49.31 ± 0.59	0.268 ± 0.005	1.5039 ± 0.0021	2.8148 ± 0.0077	0.5912 ± 0.0754	2.79 ± 0.06
8Al	448	11.76	52.78 ± 1.04	0.262 ± 0.004	1.5069 ± 0.0092	2.7892 ± 0.0015	0.655 ± 0.0277	3.1 ± 0.1

The glass transition temperature increases and the coefficient of thermal expansion decreases along with the increase of the alumina content in the glasses in accordance with a progressive increase of the average bonding strength and network reticulation. Furthermore, the elastic modulus also increases while the coefficient of Poisson becomes slightly smaller due to the increased cross-linking and dimensionality of the network [13]. The effect of network cross-linking is very well reflected in the plot of the elastic modulus *vs* the glass transition temperature as represented in Fig. 1, for which a linear relationship exists in the given compositional range.

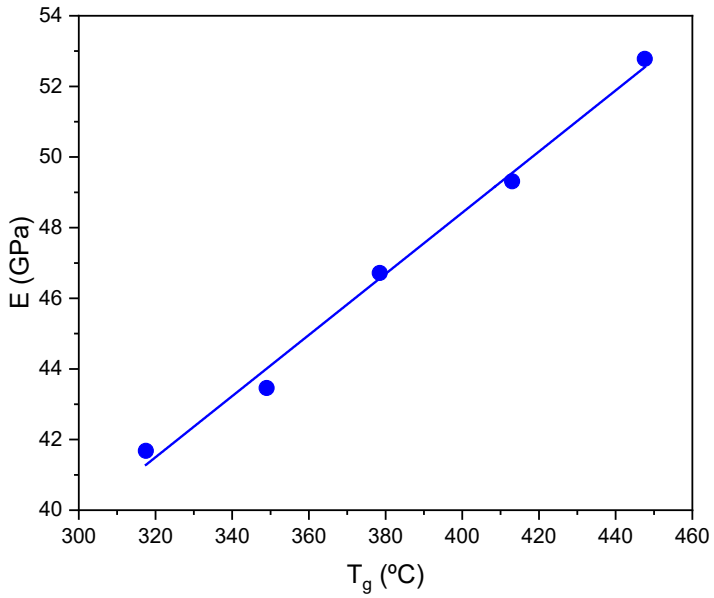

***Figure 1**. Relationship between elastic modulus, E, and glass transition temperature, T_g. Error bars are within the size of the symbols.*

On the other hand, the refractive index remains very similar for all compositions around 1.5, even though there is slight, but significant, decrease of density upon the alumina incorporation; this suggest that some other additional factor could be playing some important role.

The molar volume (V_m) has been calculated dividing the molar mass of each glass composition by the respective density, and this has been used to calculate the atomic packing density, or packing fraction C_g, through the equation below:

$$C_g = 1/V_m \times \Sigma_i x_i \cdot V_i \quad (7)$$

Where the product of the molar fraction and theoretical volume occupied by each cation and its respective oxygen coordinating shell (V_i) is divided by the glass molar volume; with $V_i = 4\pi/3 \cdot N_A \cdot (x \cdot r_A^3 + y \cdot r_B^3)$ for any oxide with composition A_xB_y. Ionic radii were takend from tabulated values in the work by Shannon in [14]. Both molar volume and packing density have been plotted in Fig. 2a and 2b, respectively. The molar volume of the glasses shows a progressive increase with the alumina addition, while the C_g slightly increases from 0 to 2 % of Al_2O_3 and then it remains almost constant or with a subtle increase only until 8 % alumina.

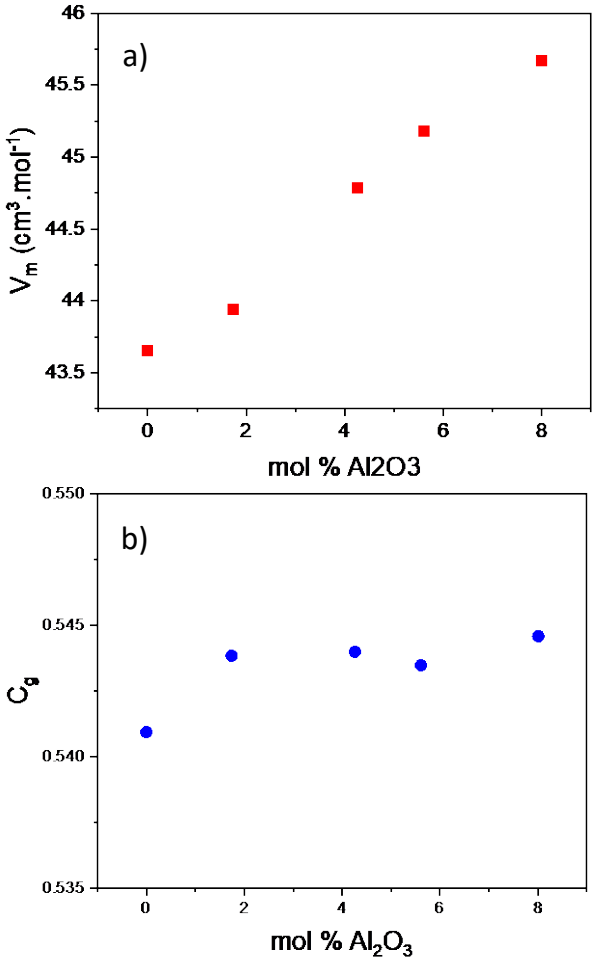

***Figure 2**. Molar volume (V_m) (a) and atomic packing density (C_g) (b) as a function of the analysed alumina content of the glasses.*

The calculation of the C_g values has been done considering that the coordination of aluminium is constant at 6 since almost all aluminium atoms would be octahedrally coordinated for the metaphosphate system. Furthermore, in the previous study of the 4 mol % Al_2O_3 glass of the same system, we found that aluminium is indeed in 6-fold coordination mainly. On the other hand, if one continues adding Al_2O_3 up to the 25 mol %, the final composition of the glass would be approaching $Al(PO_3)_3$, the aluminium metaphosphate, whose aluminium atoms are actually in 6-fold coordination. It is then thought that the incorporation of alumina, together with the increase of phosphorus that keeps the metaphosphate line constant, leads to a network structure that reaches a higher level of compaction by decreasing the free volume upon the formation of a chemical ordering similar to that of aluminium metaphosphate. Some higher fractions of 4-fold and 5-fold coordinated aluminium for the highest Al_2O_3 contents above 4 %, could indeed result in a higher degree of compaction; however, it is not thought that their content would significantly alter the present results if aluminium remains mostly in 6-fold octahedra. Meanwhile the change in packing density apparently does not present any important difference between the studied compositions, the molar volume calculated from density measurements shows a clear increase with the introduction of alumina, as well as of P_2O_5 to keep the metaphosphate ratio constant, that is consistent with a higher coordination of aluminium throughout the compositions studied. Nonetheless, the fact that the packing fraction shows some increase with respect to the 0 mol % Al_2O_3 glass may indicate the presence a counteracting effect onto the refractive index that opposes its expected variation from density measurements.

Finally, it can be noted that both the heat capacity and thermal diffusivity of the glasses increase with Al_2O_3 incorporation, which anticipates that the thermal conductivity will also be increased.

The next step before being able to calculate the thermal shock resistance of the glasses, it is to obtain the fracture toughness, which, as it was introduced above, has been approached by the model proposed by Rouxel in [4]. The fracture toughness of a typical inorganic glass can be defined as:

$$K_{Ic} = [2 \cdot \gamma \cdot E/(1-\nu^2)]^{1/2} \quad (8)$$

With E and ν the elastic modulus and coefficient of Poisson, respectively and γ the fracture surface energy that must be surpass for the associated crack growth process. Therefore, one first needs to calculate the surface energy implicated, which is done using the number and type of bonds of the given structure that must be broken in order for new surface to develop under the crack progression. The expression given for γ is:

$$\gamma = 0.5 \cdot V_m^{-1} \cdot \Sigma_i U_{<Oi>} \cdot x_i \cdot n_i \quad (9)$$

Being V_m the molar volume, $U_{<Oi>}$ the bond energy between the i^{th} element and the oxygen (in $J.mol^{-1}$), x_i the molar fraction of the element and n_i the number of bonds that must be broken per element and that has been taken as 1. The values of the bond energies have been taken from [15].

The calculated fracture toughness has been plotted against the alumina content in Fig. 3 and the inset shows the values for γ in each composition. The calculated surface energy, γ, takes very similar values for the first alumina contents while it clearly increases more significantly for 6 and 8 mol %. On the other hand, while there is a regular increase of K_{Ic} with the content of alumina, some higher increasing rate seems to take place between 4 and 8 mol % Al_2O_3 than below 4 mol %, as indicated by the linear fits of the data points between both regions, below and above 4. However, a higher impact of alumina on calculated K_{Ic} values above 4 mol % could not be regarded as truly influencing since given that the fracture surface energy has been obtained by theoretical calculation, this might be altering the obtained behavior.

Meanwhile the resistance for the crack growth experiences an increase from the beginning of alumina addition, due mainly to the higher bond energy of the Al-O bonds than of the alkali and alkaline-earth modifiers to oxygen, the fact that there is higher probability of finding Al-O-P-O-Al linkages for the highest alumina contents instead of having Al-O-P bonds separated from each other, makes the network having a much higher bonding strength that is able to hinder the crack growth in any possible direction.

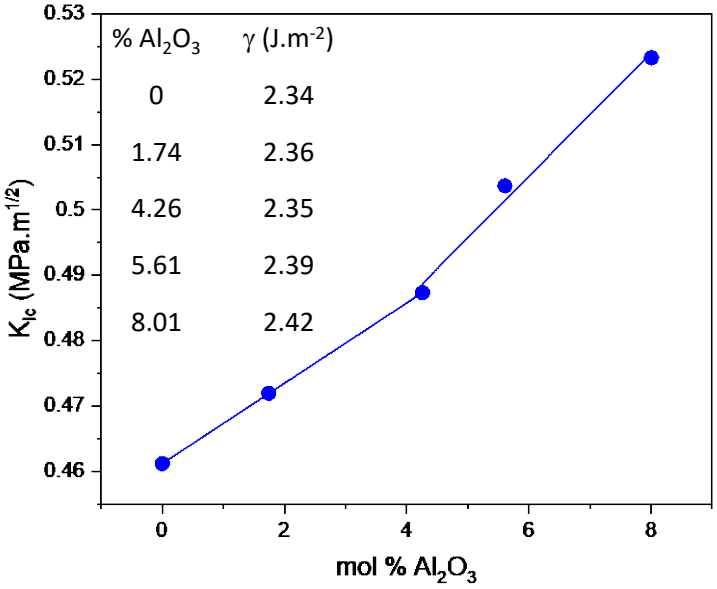

Figure 3. Fracture toughness as a function of the alumina content and values of surface energy for crack growth.

As it has been shown by Rouxel in [16], the experimentally determined fracture toughness follows a linear behaviour with the fracture surface energy that can be calculated from K_{Ic} and E measurements, being the lowest values for the chalcogenide glasses and the highest reported for the silicon oxynitride ones. The values of these studied alumino-phosphate glasses would fit very well the trend between K_{Ic} and γ relationship, adopting values between the borate and silicate glasses. Furthermore, the calculated K_{Ic} for the phosphate laser glass LG750 from Schott, whose composition is known, and the experimentally determined one agree very well, as shown in [4] within less than 10 % difference. However, a systematic comparison with experimental values in alumina-phosphate laser glasses is not easy since most glasses have proprietary compositions. The work where the theoretical approximation to the fracture surface energy is described, reference [4], showed a table with experimentally determined fracture toughness (K_{Ic}) and the theoretical one obtained from calculated fracture surface energy (γ) for a number of glasses of different systems, most being silicates. The table includes the values of γ and K_{Ic} for the proprietary laser glass Schott LG-750, having a composition similar to the one of the present study and the calculated and experimental values of K_{Ic} are 0.522 and 0.48, respectively. The difference between both is of 9 % with respect of the experimental value. In the case of the silicate systems presented in reference [4], the calculated K_{Ic} can be lower or higher than the experimental one, so this approximation is not always overestimating the fracture toughness. Meanwhile the results obtained for the calculated K_{Ic} could be introducing some higher error in the final thermal shock resistance of the glasses, there is a clear increase of the surface energy and calculated fracture toughness in agreement with the change in composition and, furthermore, the observed changes in the other properties, such that thermal expansion coefficient and thermal conductivity, are considerably higher after the incorporation of alumina. Future experimental measurements of the fracture toughness of these and similar glasses are being envisaged in order to fully characterize the systems against compositional changes.

The last step before obtaining the thermal shock resistance of the glasses is the calculation of the thermal conductivity, which is done using the equation (6) above, for which values of C_p and diffusivity at 27ºC have been used as the measuring temperature of diffusivity. Thermal conductivity has been plotted in Fig. 4 as a function of the alumina content. Overall there seems to be a near linear increase of thermal conductivity with the increase of alumina

in the glasses, that is also a reflection of the increased cross-linking density and strength of the network structure throughout which the thermal vibrations can be transmitted.

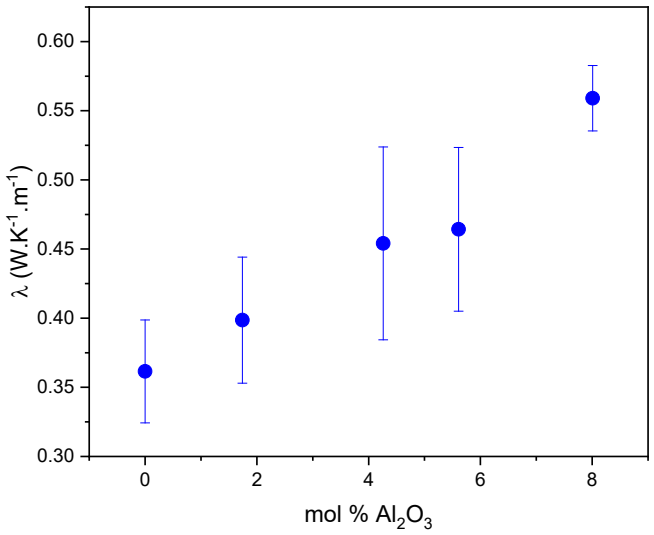

***Figure 4**. Thermal conductivity of the glasses as calculated by equation (6).*

Because the major error in the calculation of the conductivity comes from the measurements of C_p, the error bars in the data points represent the same percentage error from the standard deviation of the three heat capacity measurements at 27ºC. The variation of λ with the content of alumina could thus be assumed as linear, within the limits of error.

Finally, the thermal shock resistance of the glasses can be calculated using the expression in (1) and the result is shown in Fig. 5. Thermal conductivity, elastic modulus, coefficient of Poisson and fracture toughness have all been determined or calculated at room temperature, and the coefficient of thermal expansion has been chosen within the interval of temperature from 30ºC to 300ºC (Table 2), as it is often used when reporting thermal characteristics of phosphate laser glasses [1], [7].

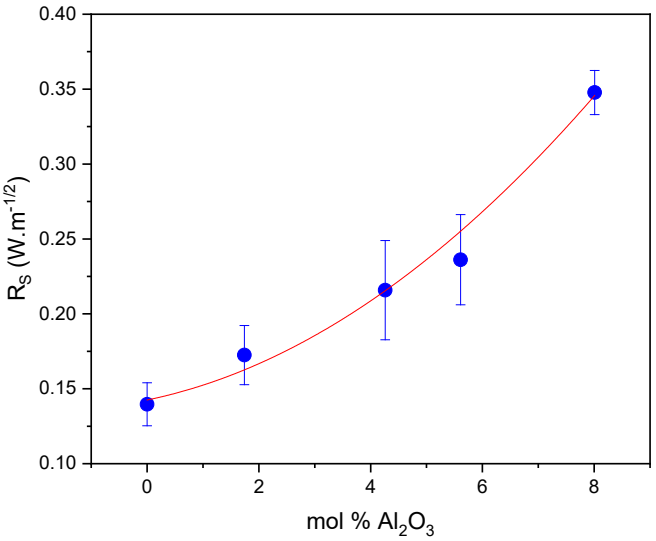

***Figure 5**. The thermal shock resistance against the alumina content calculated with equation (1). The line has been drawn as a guide for the eyes.*

Error bars in data points have again been plotted as the percentage of deviation from average similar to the one in thermal conductivity calculation. The results evidence the clear increase of the thermal shock resistance of the glasses with the increase of alumina in the metaphosphate compositions. While the variation of elastic modulus, coefficient of thermal expansion and coefficient of Poisson is linear with the alumina content, there is however a rather bigger increase of the calculated K_{Ic} values between 4 and 8 mol % Al_2O_3, than for lower contents, as principally due to the higher calculated surface energy during crack propagation, γ, in that composition range (see Fig. 3). This last could actually be at the origin for the higher increase of shock resistance between 6 and 8 % of alumina.

The thermal conductivity of the glasses seems to be, after all, one of the main properties that may control the final resistance to thermal shock during operation, being the percentage of change in λ between the lowest and highest alumina content of nearly 60 %. In this sense, high density glasses, such heavy metal oxide containing ones, could be an interesting option to study. In addition, introduction of alumina in the metaphosphate composition can indeed substantially decrease the coefficient of expansion, which decreases by 40 % in the studied glasses, thus contributing to a higher R_S. However, this may simultaneously increase the elastic modulus in an opposite effect, although in a smaller extend as shown in these glasses with a 25 % variation. Future studies of glass properties against systematic variation of composition will thus be necessary in order to find the ways to reach high thermal shock resistance values together with adequate spectroscopic properties.

4. Conclusions

Throughout the results presented in this work, we have shown that it is possible to estimate the thermal shock resistance of phosphate laser glasses upon alumina incorporation. Determination of the main thermal and elastic properties of the glasses, together with the calculated values of fracture toughness allowed us to conclude that the resistance to thermal shock increases with the increase of the content of alumina for the metaphosphate compositional line. Meanwhile the influence of alumina seen on the studied properties is linear, the calculated fracture toughness using the theoretical model proposed by Rouxel showed a higher increase of K_{Ic} for the highest alumina contents, originated by the more important values of the energy required for the fracture propagation.

Data availability statement

Data of presented results can be provided upon request.

Author contributions

Conceptualization by F.M. and R.J.J.-R.; Glass preparation and characterization by C.G., R.J.J.-R. and F.M.; Data analysis and interpretation by C.G., R.J.J.-R. and F.M.; Funding acquisition by R.J.J.-R. and F.M.; Writing, editing and review original draft by C.G., R.J.J.-R. and F.M.

Competing interests

The authors declare that they have no competing interests.

Funding

The work has been funded through projects PID2020-115419GB-C21 (LUMGLASS) and PID2021-127033OB-C21 from MCINN/AEI/10.13039/501100011033, and project ASAP-CM S2022/BMD-7434 of the Autonomous Community of Madrid.

Acknowledgement

The authors are grateful to Dr. Tanguy Rouxel for the fruitful discussions.

References

[1] J.H. Campbell, T.I. Suratwala, Nd-doped phosphate glasses for high-energy/high-peak-power lasers, J. Non-Cryst. Solids, 263&264, pp. 318-341, 2000.
[2] W.D. Kingery, Introduction to Ceramics, Wiley (New York) 1975.
[3] J.-P. Guin, Y. Gueguen, Mechanical properties of glass, in Springer Handbook of Glass, Springer Nature, Switzerland AG, 2019. Doi: 10.1007/978-3-319-93728-1.
[4] T. Rouxel, Fracture surface energy and toughness of inorganic glasses, Script. Mater. 137, 109-113, 2017, doi: 10.1016/j.scriptamat.2017.05.005.
[5] K.A. Cerqua, S.D. Jacobs, A. Lindquist, Ion-exchange strengthened laser phosphate glass, J. Non-Cryst. Solids, 93, pp. 361-376, 1987.
[6] S. Jiang, M. Myers, N. Peyghambarian, Er3+ phosphate glasses and lasers, J. Non-Cryst. Solids 239, pp. 143-148, 1998.
[7] J.H. Campbell, J.S. Hayden, A. Marker, High Power Solid-State Lasers: a Laser Glass Perspective, Int. J. App. Glass Sci. 2 (1), pp. 3-29, 2011. Doi:10.1111/j.2041-1294.2011.00044.x.
[8] Y. Cheng, C. Yu,*, H. Dong, S. Wang, C. Shao, Y. Sun, S. Sun, Y. Shen, J. Cheng, L. Hu, Spectral properties of ultra-low thermal expansion Er3+/Yb3+ co-doped phosphate glasses, Ceram. Int., 49, pp. 18305-18310, 2023. Doi:10.1016/j.ceramint.2023.02.202.
[9] F. Muñoz, R. Balda, A highly efficient method of dehydroxylation and fining of Nd phosphate laser glasses, Int. J. App. Glass Sci. 10, pp.157-161, 2019. Doi: 10.1111/ijag.12974.
[10] M. Muñoz-Quiñonero, J. Azkargorta, I. Iparraguirre, R.J. Jiménez-Riobóo, G. Tricot, C. Shao, F. Muñoz, J. Fernández, R. Balda, Dehydroxylation processing and lasing properties of a Nd alumino-phosphate glass, Journal of Alloys and Compounds 896, pp.163040, 2022. Doi: 10.1016/j.jallcom.2021.163040.
[11] J.K. Krüger, in Brillouin Spectroscopy and its application to Polymers in Optical techniques to characterize polymer systems, Elsevier, Amsterdam, 1989.
[12] G. Grimvall, in Thermophysical Properties of Materials, ed. E. P. Wohlfarth, North-Holland, Amsterdam, 1986.
[13] T. Rouxel, Elastic Properties and Short-to Medium-Range Order in Glasses, J. Am. Ceram. Soc., 90, 10, pp. 3019–3039, 2007. Doi: 10.1111/j.1551-2916.2007.01945.x.
[14] R.D. Shannon, Revised effective ionic radii and systematic studies of interatomic distances in halides and chalcogenides, Act. Cryst. A32, 751-767, 1976.
[15] R. Lide, Handbook of Chemistry and Physics, 88th Ed. Taylor&Francis, 2007-2008.
[16] T. Rouxel, What can we learn from crystals about the mechanical properties of glass. J. Ce-ram. Soc. Japan, 130, 8, pp. 519-530, 2022 doi:10.2109/jcersj2.22067.